JOURNAL OF APPLIED CRYSTALLOGRAPHY

ISSN 1600-5767

Single-crystal neutron diffraction in diamond anvil cells with hot neutrons

Andrzej Grzechnik,[a]* Martin Meven[a,b] and Karen Friese[c]

[a]Institute of Crystallography, RWTH Aachen University, Jaegerstrasse 17–19, 52066 Aachen, Germany, [b]Jülich Centre for Neutron Science (JCNS), Forschungszentrum Jülich GmbH at Heinz Maier-Leibnitz Zentrum (MLZ), 85748 Garching, Germany, and [c]Jülich Centre for Neutron Science-2 (JCNS-2), Forschungszentrum Jülich GmbH, 52425 Jülich, Germany. *Correspondence e-mail: grzechnik@xtal.rwth-aachen.de

Received 10 August 2017
Accepted 16 January 2018

Edited by D. Pandey, Indian Institute of Technology (Banaras Hindu University), Varanasi, India

Keywords: hot neutrons; single-crystal diffraction; diamond anvil cells; high pressure.

Supporting information: this article has supporting information at journals.iucr.org/j

It is demonstrated that it is possible to perform single-crystal measurements in diamond anvil cells (DACs) with a monochromatic beam at modern hot neutron sources that offer the benefit of short neutron wavelengths with high fluxes. A piston–cylinder DAC with conical Boehler–Almax diamonds that allows for a wide accessibility of the reciprocal space has been developed. The diffraction data collected in this cell using hot neutrons are of very good quality and can be used for a full and reliable structure refinement.

1. Introduction

Neutron scattering studies on large single crystals of several cubic millimetres are frequently performed in gas-pressure and clamp cells (Klotz, 2013; Ridley & Kamenev, 2014). There have been relatively few efforts to use other high-pressure devices for single-crystal neutron measurements. Paris–Edinburgh presses with a very restricted access to the reciprocal space are too cumbersome to be easily operated during the measurements of single-crystal intensities (Fang *et al.*, 2010). Nevertheless, they can give data suitable for structure refinement at short neutron wavelengths (Bull *et al.*, 2011). Because of the large volumes required for neutron single-crystal diffraction up to now (>1 mm^3), panoramic opposed-anvil cells with large anvils made of sapphire (Kuhs *et al.*, 1989, 1996; McMahon *et al.*, 1990) or moissanite (Xu *et al.*, 2002; McIntyre *et al.*, 2005) have been employed to collect data for full structure refinement.

A diamond anvil cell (DAC) is the most versatile tool in high-pressure technology and allows the combination of numerous experimental techniques to study various states of matter under compression (*e.g.* X-ray diffraction and absorption, vibrational and optical spectroscopies, *etc.*). DACs have also been used for neutron powder diffraction (Boehler *et al.*, 2013; Goncharenko, 2004, 2007; Guthrie *et al.*, 2013, 2017; Okuchi *et al.*, 2014). Their major limitation for neutron scattering on single crystals is the sample volume, which is typically much smaller than 1 mm^3. Some opposed-anvil cells could be modified to accommodate diamonds (Besedin *et al.*, 1990, 1995; Goncharenko, 2004, 2007). For instance, the cells used for the studies of single crystals of deuterium to 31 GPa by Besedin *et al.* (1990) and to 38 GPa by Goncharenko & Loubeyre (2005) were equipped with diamonds that had culets of 0.7 and 0.6 mm, respectively. In both cases, only seven reflections were measured to determine solely the equation of state but not to perform any structural refinement. Recently, Binns *et al.* (2016) have shown that neutron Laue diffraction

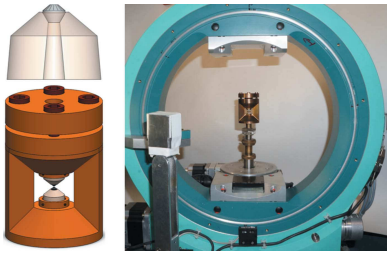

from very small crystals (about 0.01 mm^3) in Merrill–Bassett diamond anvil cells (Merrill & Bassett, 1974) provides high-quality data for structure determination and refinement.

The goal of our present study is to investigate whether single-crystal measurements in diamond anvil cells are also feasible with a monochromatic beam at modern hot neutron sources that offer the benefit of short neutron wavelengths with high fluxes. For this purpose, we have started using the single-crystal diffractometer HEiDi at the Heinz Maier-Leibnitz Zentrum (MLZ) in Garching. HEiDi is a four-circle diffractometer (HUBER) and operates at different monochromatic wavelengths between $\lambda = 0.556$ Å and $\lambda = 1.170$ Å with high fluxes (*e.g.* 3×10^6 n cm^{-2} s^{-1} at $\lambda = 0.556$ Å and 1.4×10^7 n cm^{-2} s^{-1} at $\lambda = 1.17$ Å; Meven & Sazonov, 2015). The diffracted intensities are collected with a point detector optimized for small wavelengths (sensitivity >90% at 0.3 Å). The minimal volume of single crystals that can be studied on pins in the air without any sample environment depends on the structure factor $F(000)$, *i.e.* the structure factor in the zero-order case $h = k = l = 0$ at $\theta = 0°$, scaled with the unit-cell volume (V). $F(000)$ is either positive or negative for neutrons and counts the total nuclear scattering power in the unit cell. For high ratios of $|F(000)|/V$ of about 0.5 $Å^{-3}$ and the high neutron fluxes available at HEiDi, it is possible at present to measure crystals smaller than 0.1 mm^3. Already available sample environments permit investigations on larger crystals at temperatures between 2.5 and 1300 K or in an electric field.

It should be pointed out that the Q range becomes larger for short neutron wavelengths. This is especially important in a high-pressure experiment where the opening angles of the DAC limit the accessibility of the reciprocal space. A further advantage of high neutron energies is the minimization of absorption effects not only of crystals containing strong absorbers like Gd, Dy, Sm *etc*. but also of the sample environment. The fact that the neutrons can easily penetrate the materials in the sample environment opens the possibility to use the DAC both in the transmission geometry (Binns *et al.*, 2016) and in the panoramic mode, in which the incident and diffracted beams pass through the gasket material only.

2. Diamond anvil cells and experimental data

Our first trial measurements on HeiDi were performed at room temperature in the panoramic diamond anvil cell designed for X-ray diffraction by Ahsbahs (1984) (Fig. 1). Modified versions of this cell, which also include sapphire anvils, have been used for neutron diffraction by Kuhs *et al.* (1989, 1996) and McMahon *et al.* (1990), and by Guionneau *et al.* (2004) for X-ray diffraction. For our experiment on HEiDi, the cell was loaded with a crystal of $MnFe_4Si_3$ (the crystal size of $0.5 \times 0.6 \times 0.9$ mm $\simeq 0.3$ mm^3), ruby and a 4:1 mixture of deuterated methanol:ethanol as pressure medium. The pressure was determined using ruby luminescence. The seats for the diamond anvils (the culet diameter of 1.5 mm) made of steel were coated with nail polish mixed with a fine powder of Gd_2O_3 (the Gd paint) in order to suppress the parasitic Bragg scattering from the steel. The gasket material (10 mm in diameter and 2 mm in thickness) was Berylco25 (CuBe). It was pre-indented to about 1.2 mm. The diameter of the hole in the gasket was 0.8 mm. The orientation matrix of the hexagonal crystal was determined before the experiment on an in-house laboratory X-ray Laue camera. The measurements ($\lambda = 1.17$ Å) were performed at ambient pressure and at 1.0 GPa. In both cases, we were able to find reflections of the sample using the standard routines for searching reflections in the reciprocal space with a point detector. Two hundred reflections were collected at ambient pressure, while nearly three hundred reflections were measured at 1.0 GPa (Table 1). The average measuring time was about 13 minutes per reflection.

Reducing the beam size with slits allowed us to considerably minimize the background, which can be attributed to different components of the diamond anvil cell (*e.g.* three posts in the cell). We also note that the signal-to-noise ratio for the

Table 1
Experimental data on $MnFe_4Si_3$ ($P6_3/mcm$, $Z = 2$) at 1.0 GPa in two different diamond anvil cells.

	Ahsbahs cell	Our cell
Crystal data		
a (Å)	6.80 (1)	6.80 (1)
c (Å)	4.75 (1)	4.75 (4)
V ($Å^3$)	190.2	190.2
ρ (g cm^{-3})	6.33	6.33
Data collection		
No. of measured reflections	293	831
Range of hkl	$0 \le h \le 7$	$-8 \le h \le 8$
	$-5 \le k \le 6$	$-8 \le k \le 8$
	$-5 \le l \le 6$	$-4 \le l \le 5$
No. of observed reflections†	50	52
$R(\text{int})_{\text{obs}}$‡	26.27	10.62
Redundancy	2.6	13.8
Refinement‡		
R_{obs}	12.74	7.83
wR_{obs}	11.34	6.12
GoF_{obs}	3.35	3.15
No. of parameters	6	12

† Criterion for observed reflections is $|F_{\text{obs}}| > 3\sigma$. ‡ All agreement factors are given in %, weighting scheme is $1/[\sigma^2(F_{\text{obs}}) + (0.01F_{\text{obs}})^2]$.

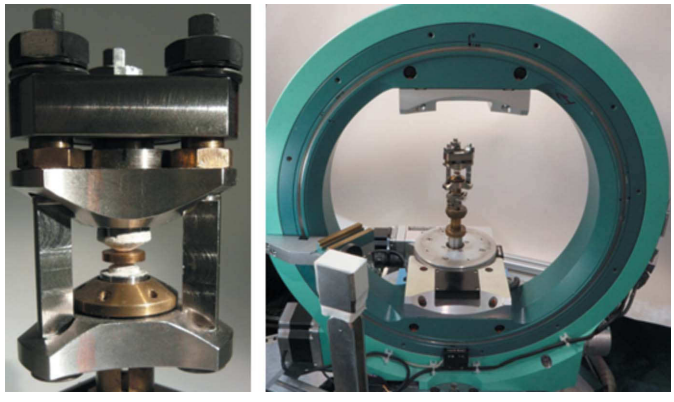

Figure 1
Ahsbahs-type panoramic diamond anvil cell (left) installed on the four-circle HUBER diffractometer at HEiDi (right).

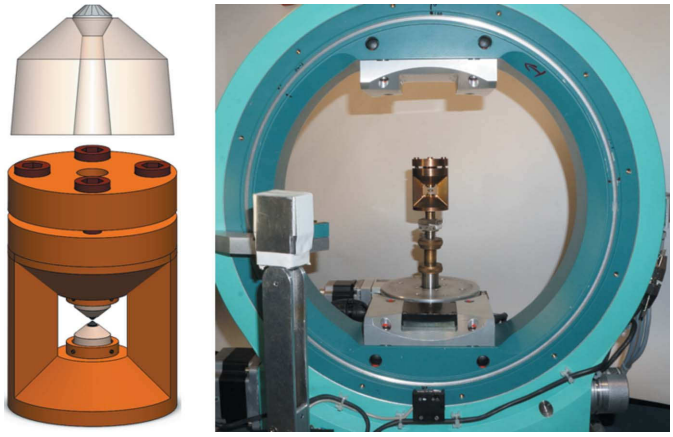

Figure 2
The panoramic diamond anvil cell developed in this study (bottom left) installed on the four-circle HUBER diffractometer at HEiDi (right). The cell diameter is 45 mm. Each of the two horizontal openings is equal to 135°. The top-left drawing shows a seat with a conical Boehler–Almax diamond.

measured reflections improved significantly when using higher energies, *i.e.* when using hotter neutrons ($\lambda < 1.0$ Å), owing to the reduced scattering/absorption of the neutron beam by the CuBe gasket. This clearly proves the usefulness of hot neutrons for single-crystal measurements on small crystals in diamond anvil cells.

On the basis of the promising results of our first experiments, we have now developed a panoramic piston–cylinder DAC (Fig. 2) that includes conical Boehler–Almax diamonds of type 1a with an aperture of 30° (Boehler & De Hantsetters, 2004) using the software *SOLIDWORKS* (Dassault Systèmes; http://www.solidworks.com/). It is a modification of the types by Ahsbahs (1984) and Goncharenko (2004, 2007). This two-post cell has two horizontal (and symmetrical) openings of 135° (cells with openings of 150° could also be produced). The vertical angular opening is 80°. The horizontal and vertical openings allow for a wide accessibility of the reciprocal space. Conical openings in the seats as well as in the piston and cylinder along the cell axis allow for optical access to the sample. They permit the pressure calibration with ruby luminescence and other spectroscopic measurements. Presently, the entire cell body and the diamond seats are made of CuBe. Parallel alignment of the diamond anvils is obtained owing to the precision manufacture of the cell body and the seats. The cells can be produced in various sizes (40–50 mm in diameter, 60–75 mm in height) to be gas-membrane driven and to fit into the standard cryostats available at the MLZ in Garching.

To characterize and optimize the performance of the cell, finite element analysis (FEA) was carried out using the simulation package in the software *SOLIDWORKS*. Representative results are shown in Fig. 3. We define the factor of safety (FoS) as a ratio of the yield stress (σ_y) of the material used to manufacture our cell to the working stress. Accordingly, the cell would start to fail when the elastic limit of any of its components was exceeded by the working stress (FoS < 1). As can be seen from the left part of Fig. 3, the component most prone to failure is the diamond seat at its tip. The analysis also allows us to find the critical (or average) pressure on the diamond culet, *i.e.* the pressure at which FoS = 1 for any component of the cell (Fig. 3, right). Note that the maximum pressure that can effectively be reached in the sample chamber is much higher than this average pressure. According to Sadkov & Solodukhina (1993) and Jin *et al.* (2017), the actual pressure limit could be three times as high as that determined from the finite element analysis, providing the diamond anvils withstand these conditions. Thus, for a culet diameter of 1 mm, a critical (FEA) pressure limit for the cell of about 4 GPa (Fig. 3) would correspond to an actual pressure of approximately 12 GPa at the sample. We performed tests with our cell up to about 7 GPa for diamonds of this size and did not observe any damage to the seats and the anvils. However, we did not attempt to reach higher pressures in these tests to avoid breaking the diamonds.

The data collection strategy in our DAC at room temperature was similar to that in the Ahsbahs-type cell. Another but smaller $MnFe_4Si_3$ crystal (0.4 × 0.5 × 0.9 mm ≃ 0.2 mm^3), pre-oriented with the X-ray Laue technique, and a ruby were loaded into our DAC with a 4:1 mixture of deuterated methanol:ethanol as pressure medium. The pressure of 1.0 GPa was determined using ruby luminescence. The seats for the diamond anvils (with a culet diameter of 1.0 mm) were coated with Gd paint. The CuBe gasket (8 mm in diameter and 1.5 mm in thickness) was pre-indented to about 1.1 mm. The diameter of the hole in the gasket was 0.6 mm. Over 800 diffracted intensities were collected (λ = 1.17 Å) with an

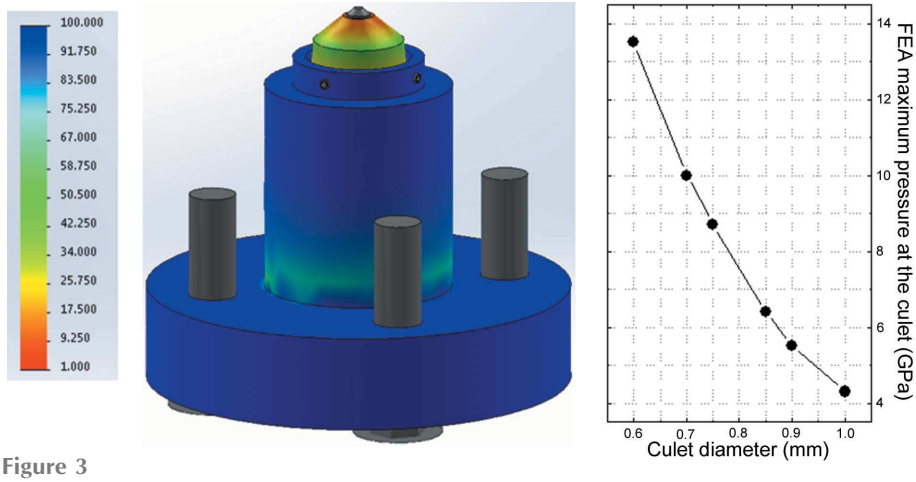

Figure 3
Results of the finite element analysis of the piston assembly in the cell of Fig. 2: (left) the factor-of-safety distribution, (right) the highest (critical) pressure that could be applied to the diamonds with different culet sizes when FoS = 1. The line is a guide for the eye. The yield stress for CuBe is σ_y = 1169 N mm^{-2}.

Table 2
Refined structural parameters for $MnFe_4Si_3$.

Data shown in bold and in normal fonts were obtained at 1.0 GPa in our panoramic and Ahsbahs cells, respectively. Data shown in italics were obtained using neutron single-crystal diffraction at 380 K and ambient pressure (Hering *et al.*, 2015).

Atom	Occupancy	x	y	z	U_{eq}
Mn1	**0.30 (3)**	**0.7577 (16)**	**0.7577 (16)**	**0.25**	**0.017 (5)**
	0.3333	0.7592 (20)	0.7592 (20)	0.25	0.018 (3)
	0.316 (4)	*0.7580 (4)*	*0.7580 (4)*	*0.25*	*0.0084 (10)*
Fe1	**0.70 (3)**	**0.7577 (16)**	**0.7577 (16)**	**0.25**	**0.017 (5)**
	0.6667	0.7592 (20)	0.7592 (20)	0.25	0.018 (3)
	0.684 (4)	*0.7580 (4)*	*0.7580 (4)*	*0.25*	*0.0084 (10)*
Fe2	**1**	**0.6667**	**0.3333**	**0**	**0.0101 (19)**
	1	0.6667	0.3333	0	0.016 (2)
	1	*0.6667*	*0.3333*	*0*	*0.0058 (7)*
Si	**1**	**0.3997 (16)**	**0.3997 (16)**	**0.25**	**0.011 (6)**
	1	0.4020 (24)	0.4020 (24)	0.25	0.018 (4)
	1	*0.3997 (5)*	*0.3997 (5)*	*0.25*	*0.0068 (10)*

Atom	U_{11}	U_{22}	U_{33}	U_{12}	U_{13}	U_{23}
Mn1	**0.022 (5)**	**0.022 (5)**	**0.009 (11)**	**0.012 (5)**	**0**	**0**
	0.0056 (13)	*0.0056 (13)*	*0.0119 (15)*	*0.0013 (11)*	*0*	*0*
Fe1	**0.022 (5)**	**0.022 (5)**	**0.009 (11)**	**0.012 (5)**	**0**	**0**
	0.0056 (13)	*0.0056 (13)*	*0.0119 (15)*	*0.0013 (11)*	*0*	*0*
Fe2	**0.0105 (18)**	**0.0105 (18)**	**0.009 (4)**	**0.0052 (9)**	**0**	**0**
	0.0055 (9)	*0.0055 (9)*	*0.0064 (10)*	*0.0027 (4)*	*0*	*0*
Si	**0.011 (5)**	**0.011 (5)**	**0.011 (13)**	**0.006 (5)**	**0**	**0**
	0.0046 (12)	*0.0046 (12)*	*0.0103 (14)*	*0.0017 (12)*	*0*	*0*

average measuring time of about eight minutes per reflection (Table 1).

The direct and diffracted beams were corrected for the attenuation due to the gasket using a procedure similar to that adopted by Kuhs *et al.* (1989). The path of the beams depends on the angle γ, which is defined as $\gamma = \arcsin(\sin\theta \sin\chi)$, where θ and χ are the Eulerian angles of the four-circle diffractometer. The maximum value of the γ angle is half of the horizontal opening of the DAC, *i.e.* $|2\gamma| \leq 80°$ in our cell. The attenuation due to the diamond anvils was excluded from the correction since its linear attenuation factor (cm^{-1}) as a function of the wavelength λ (Å), $\mu_{diamond} = 0.0005\lambda$, is negligible compared to that for CuBe, $\mu_{CuBe} = 0.1611\lambda + 0.042$ (Binns *et al.*, 2016). The calculated attenuation correction factors vary nonlinearly with γ and their relative change is about 13% (Fig. 4).

The diffracted intensities from $MnFe_4Si_3$ at 1.0 GPa, corrected for the gasket attenuation, were further analysed with the program *Jana2006* (Petricek *et al.*, 2014) using the approach for processing of high-pressure single-crystal X-ray data described by Friese *et al.* (2013). The reflections shaded by the two posts of the DAC were identified and rejected.

To prove the suitability and reliability of our experimental setup and to evaluate the quality of the collected intensities, we refined the structure of $MnFe_4Si_3$ from the data measured in our panoramic cell. Previously, a structural model for this compound has been given in space group $P\bar{6}$ ($Z = 2$) by Hering *et al.* (2015). The structure has a high pseudo-symmetry with respect to $P6_3/mcm$ ($Z = 2$) and it is straightforward to derive a model for an average structure in this space group. Consequently, we used this average structural model for the refinement of our high-pressure data as the weak reflections violating the extinction rules of space group $P6_3/mcm$ could not be reliably observed owing to the elevated background in the high-pressure experiment. In this model, there are three symmetrically independent sites: *M*1 at the Wyckoff position 6*g*, *M*2 at the Wyckoff position 4*d* and Si at the Wyckoff position 6*g*. The site *M*1 is partially occupied by Mn and Fe, while the site *M*2 is occupied by Fe. The refined parameters were the atomic coordinates and anisotropic displacement parameters for all the atomic sites. We also attempted to refine the occupations of the *M*1 and *M*2 sites and could confirm that the *M*1 site is the only mixed Mn/Fe site, whereas the other two are fully occupied by Fe and Si, respectively. The refinement of the site occupancies yields a composition that essentially agrees with the nominal formula $MnFe_4Si_3$ within the estimated standard deviations (Tables 1 and 2). Regarding the occupancy parameters and the atomic coordinates, our results are within errors identical to those obtained from the neutron data outside the diamond anvil cell measured at 380 K (space

Table 3
Selected interatomic distances (in Å) in $MnFe_4Si_3$ at 1.0 GPa in two different diamond anvil cells and at 380 K (Hering *et al.*, 2015).

		Ahsbahs cell	Our cell	Hering *et al.* (2015)
Mn1—Mn1	2×	2.84 (2)	2.853 (18)	2.851 (3)
Mn1—Mn1	4×	2.88 (2)	2.89 (3)	2.884 (3)
Mn1—Fe2	4×	2.89 (2)	2.887 (16)	2.888 (2)
Mn1—Si1		2.43 (2)	2.435 (15)	2.438 (3)
Mn1—Si1	2×	2.38 (3)	2.37 (2)	2.373 (6)
Mn1—Si1	2×	2.62 (1)	2.61 (4)	2.600 (1)
Fe2—Fe2	2×	2.38 (1)	2.38 (4)	2.3678 (1)
Fe2—Si1	6×	2.39 (2)	2.393 (15)	2.393 (3)
Si1—Si1	2×	2.72 (1)	2.74 (4)	2.733 (2)

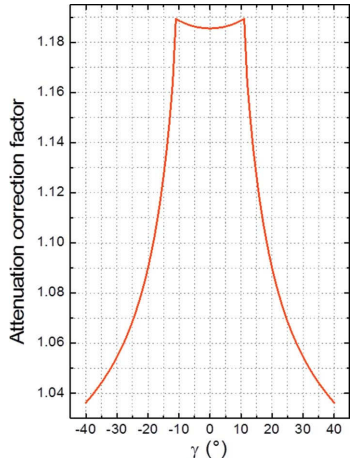

Figure 4
Attenuation correction factors as a function of the γ angle for the CuBe gasket and wavelength (λ = 1.17 Å) used in this study.

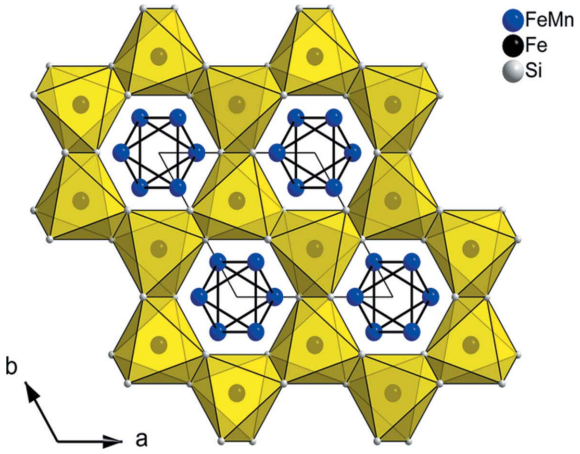

Figure 5
Crystal structure of $MnFe_4Si_3$ at 1.0 GPa. The Fe_2Si_6 octahedra are drawn in yellow.

group $P6_3/mcm$, $Z = 2$) on the beamline R42 (TriCS) in the SINQ spallation source of the Paul Scherrer Institute (Hering *et al.*, 2015). Selected interatomic distances and the crystal structure of $MnFe_4Si_3$ at 1.0 GPa are listed in Table 3 and shown in Fig. 5, respectively. The distances derived from our present data and from the data measured at TriCS are essentially the same. All this proves that reliable structure determination and refinement with monochromatic hot neutrons at high pressures using our cell are indeed possible.

The data collected at the Ahsbahs-type cell at ambient conditions and 1.0 GPa could only be refined when the displacement parameters for all the sites are isotropic and the Mn1/Fe1 occupancies are fixed to the nominal ones (Table 2). The reason is that the number of measured reflections is much lower because of the smaller opening angles in this three-post cell (Ahsbahs, 1984), *i.e.* as a result of a narrower accessibility of the reciprocal space. The angle between the two neighbouring posts is slightly less than 120°. During the neutron data collection, the effective opening angle is much smaller owing to the presence of the third post, partially obscuring the incident beam and affecting the diffracted intensities. This results in high values of the $R(\mathrm{int})_{\mathrm{obs}}$ and R_{obs} factors as well as in the low redundancy for this data set (Table 1).

3. Outlook

Our studies on HEiDi at MLZ clearly demonstrate that the single-crystal neutron diffraction data collected in diamond anvil cells using hot neutrons are of very good quality and can be used for a full and reliable structure refinement. In the near future, we would like to extend the measurable pressure range, thus exploiting the potential of our DAC to a much higher extent. One of the key factors for this is to enhance the neutron flux at the sample position for short wavelengths. For this, we plan to increase the reflectivity of the Cu220 monochromator through a special thermal treatment. In addition, we will improve the signal-to-noise ratio by optimizing the primary beam optics. These future developments will permit us not only to perform single-crystal neutron studies at moderate pressures of several GPa but also to study samples with volumes much smaller than 0.1 mm^3.

Acknowledgements

We thank Hans Ahsbahs for his diamond anvil cell and for several fruitful discussions. Micha Hölzle has been helping us with manufacturing our cells. Vladimir Hutanu and Hao Deng have been sharing their knowledge of hot neutrons with us. Wolfgang Luberstetter, Philipp Tesch and Paul Zakalek have assisted us with data collection and processing. The HEiDi instrument at the Heinz Maier-Leibnitz Zentrum (MLZ) in Garching (Germany) is jointly operated by the Institute of Crystallography (RWTH Aachen University) and the Jülich Centre for Neutron Science (Forschungszentrum Jülich) within the Jülich Aachen Research Alliance (JARA).

Funding information

This work is supported by the project 05K16PA3 from the Bundesministerium für Bildung und Forschung (BMBF) (to Georg Roth, Martin Meven and Andrzej Grzechnik).

References

Ahsbahs, A. (1984). *Rev. Sci. Instrum.* **55**, 99–102.
Besedin, S. P., Makarenko, I. N., Stishov, S. M., Glazkov, V. P., Goncharenko, I. N., Irodova, A. V., Somenkov, V. A. & Shil'stein, S. S. (1990). *High Pressure Res.* **4**, 447–449.
Besedin, S. P., Makarenko, I. N., Stishov, S. M., Glazkov, V. P., Goncharenko, I. N. & Somenkov, V. A. (1995). *High Pressure Res.* **14**, 193–197.
Binns, J., Kamenev, K. V., McIntyre, G. J., Moggach, S. A. & Parsons, S. (2016). *IUCrJ*, **3**, 168–179.
Boehler, R. & De Hantsetters, K. (2004). *High Pressure Res.* **24**, 391–396.
Boehler, R., Guthrie, M., Molaison, J. J., dos Santos, A. M., Sinogeikin, S., Machida, S., Pradhan, N. & Tulk, C. A. (2013). *High Pressure Res.* **33**, 546–554.
Bull, C. L., Guthrie, M., Archer, J., Fernandez-Diaz, M.-T., Loveday, J. S., Komatsu, K., Hamidov, H. & Nelmes, R. J. (2011). *J. Appl. Cryst.* **44**, 831–838.
Fang, J., Bull, C. L., Hamidov, H., Loveday, J. S., Gutmann, M. J., Nelmes, R. J. & Kamenev, K. V. (2010). *Rev. Sci. Instrum.* **81**, 113901.
Friese, K., Grzechnik, A., Posse, J. M. & Petricek, V. (2013). *High Pressure Res.* **33**, 196–201.
Goncharenko, I. N. (2004). *High Pressure Res.* **24**, 193–204.
Goncharenko, I. N. (2007). *High Pressure Res.* **27**, 183–188.
Goncharenko, I. N. & Loubeyre, P. (2005). *Nature*, **435**, 1206–1209.
Guionneau, P., Pévelen, D. L., Marchivie, M., Pechev, S., Gaultier, J., Barrans, Y. & Chasseau, D. (2004). *J. Phys. Condens. Matter*, **16**, S1151–S1159.
Guthrie, M., Boehler, R., Molaison, J. J., dos Santos, A. M. & Tulk, C. A. (2013). *Am. Crystallogr. Assoc. Trans. Ser.* **44**, 149–169.
Guthrie, M., Pruteanu, C. G., Donnelly, M.-E., Molaison, J. J., dos Santos, A. M., Loveday, J. S., Boehler, R. & Tulk, C. A. (2017). *J. Appl. Cryst.* **50**, 76–86.
Hering, P., Friese, K., Voigt, J., Persson, J., Aliouane, N., Grzechnik, A., Senyshyn, A. & Brückel, T. (2015). *Chem. Mater.* **27**, 7128–7136.
Jin, H., Woodall, C. H., Wang, X., Parsons, S. & Kamenev, K. V. (2017). *Rev. Sci. Instrum.* **88**, 035103.
Klotz, S. (2013). *Techniques in High Pressure Neutron Scattering*. Boca Raton: CRC Press.

Kuhs, W. F., Ahsbahs, H., Londono, D. & Finney, J. L. (1989). *Physica B*, **156–157**, 684–687.
Kuhs, W. F., Bauer, F. C., Hausmann, R., Ahsbahs, H., Dorwarth, R. & Hölzer, K. (1996). *High Pressure Res.* **14**, 341–352.
McIntyre, G. J., Mélési, L., Guthrie, M., Tulk, C. A., Xu, J. & Parise, J. B. (2005). *J. Phys. Condens. Matter*, **17**, S3017–S3024.
McMahon, M. I., Nelmes, R. J., Kuhst, W. F., Dorwarth, R., Piltz, R. O. & Tun, Z. (1990). *Nature*, **348**, 317–319.
Merrill, L. & Bassett, W. A. (1974). *Rev. Sci. Instrum.* **45**, 290–294.
Meven, M. & Sazonov, A. (2015). *J. Large-Scale Res. Facil.* **1**, A7.
Okuchi, T., Tomioka, N., Purevjav, N., Abe, J., Harjo, S. & Gong, W. (2014). *High Pressure Res.* **34**, 273–280.
Petricek, V., Dusek, M. & Palatinus, L. (2014). *Z. Kristallogr.* **229**, 345–352.
Ridley, C. J. & Kamenev, K. V. (2014). *Z. Kristallogr.* **229**, 171–199.
Sadkov, Y. A. & Solodukhina, L. B. (1993). *J. Appl. Mech. Tech. Phys.* **33**, 903–910.
Xu, J. A., Mao, H. K., Hemley, R. J. & Hines, E. (2002). *J. Phys. Condens. Matter*, **14**, 11543–11548.